

SCIENTIFIC REPORTS



OPEN

Modeling the interplay between the HIF-1 and p53 pathways in hypoxia

Chun-Hong Zhou^{1,2}, Xiao-Peng Zhang³, Feng Liu^{2,4} & Wei Wang^{1,4}

Received: 29 April 2015

Accepted: 10 August 2015

Published: 08 September 2015

Both the hypoxia-inducible factor-1 (HIF-1) and tumor suppressor p53 are involved in the cellular response to hypoxia. How the two transcription factors interact to determine cell fates is less well understood. Here, we developed a network model to characterize crosstalk between the HIF-1 and p53 pathways, taking into account that HIF-1 α and p53 are targeted for proteasomal degradation by Mdm2 and compete for binding to limiting co-activator p300. We reported the network dynamics under various hypoxic conditions and revealed how the stabilization and transcriptional activities of p53 and HIF-1 α are modulated to determine the cell fate. We showed that both the transrepression and transactivation activities of p53 promote apoptosis induction. This work provides new insight into the mechanism for the cellular response to hypoxia.

Hypoxia, a decrease in oxygen availability, affects both physiological development and tumorigenesis¹. A key mediator of the cellular response to hypoxia is the hypoxia-inducible factor-1 (HIF-1), which is a heterodimer of α and β subunits. HIF-1 β is constitutively expressed, while HIF-1 α is regulated in an oxygen-dependent manner². HIF-1 α is inactive and remains at low levels in normoxia. With enough oxygen available, the hydroxylation of HIF-1 α by PHD (prolyl hydroxylase domain protein) promotes its degradation by pVHL (von Hippel-Lindau protein)³, and the hydroxylation of HIF-1 α by FIH-1 (factor inhibiting HIF-1) represses its transcriptional activity via preventing the recruitment of co-activator p300⁴. In hypoxia, both PHD and FIH-1 are deactivated, and thus HIF-1 α is stabilized and activated. As a transcription factor, HIF-1 induces expression of target genes such as VEGF (vascular endothelial growth factor), EPO (erythropoiesis) and p21^{5,6}. VEGF and EPO regulate adaptive responses to hypoxia, while p21 induces cell-cycle arrest.

The tumor suppressor p53 also mediates the hypoxic response. p53 is kept at basal levels in unstressed cells because of Mdm2-mediated ubiquitination and proteasomal degradation. The p53 response to hypoxia is diverse, depending on the cell type, the degree and duration of hypoxia⁷. For example, p53 is stabilized via phosphorylation by the ATR (ataxia-telangiectasia mutated and Rad3-related) kinase only under severe hypoxia⁸. Moreover, high levels of p53 can induce apoptosis in a different manner from that when it is activated by DNA damage^{9,10}. Notably, different mechanisms have been proposed for p53-mediated apoptosis in hypoxia: p53 promotes apoptosis mainly by transrepressing antiapoptotic genes like microRNA(miR)-17-92^{11,12}, or by transactivating proapoptotic genes such as *puma* (p53-upregulated mediator of apoptosis), *fas* and *bnip3*^{13–15}. An issue naturally arises concerning whether these mechanisms are mutually exclusive or can be coordinated in one setting.

There exists an intricate interplay between p53 and HIF-1 α . It was proposed that p53 stabilization is dependent on HIF-1 α ¹⁶; HIF-1 α may bind to Mdm2, inhibiting Mdm2-dependent degradation of p53¹⁷.

¹National Laboratory of Solid State Microstructures and Department of Physics, Nanjing University, Nanjing 210093, China. ²School of Physics and Electronic Engineering, Jiangsu Normal University, Xuzhou 221116, China. ³Kuang Yaming Honors School, Nanjing University, Nanjing 210093, China. ⁴Collaborative Innovation Center of Advanced Microstructures, Nanjing University, Nanjing 210093, China. Correspondence and requests for materials should be addressed to X.-P.Z. (email: zhangxp@nju.edu.cn) or F.L. (email: fliu@nju.edu.cn)

Regulation of HIF-1 α activity. In normoxia, HIF-1 α is kept at low levels due to oxygen-dependent hydroxylation that promotes its degradation by pVHL³. HIF-1 α can also be degraded by Mdm2 in a p53-dependent manner²². Under hypoxic conditions, the hydroxylation of HIF-1 α drops remarkably, and HIF-1 α accumulates. HIF-1 α dimerises with HIF-1 β in the nucleus. p300/CBP promotes the acetylation of HIF-1 α , enhancing its transcriptional activity. In our model, HIF-1 α is divided into unacetylated (HIF-1 α , inactive) and acetylated (HIF-1 α_{ac} , active) forms, and their conversion is controlled by p300. The amount of p300 is limited¹⁸ and is set to a constant in the standard parameter setting. Because they can bind to p300 at different sites^{23,24}, HIF-1 α and p53 compete for limiting p300, the modeling of which is described later. Given the inhibitory effect of acetylation on protein degradation, only unacetylated HIF-1 α is degraded through the PHD- or Mdm2-dependent mechanism²². The degradation and (de)acetylation processes are taken as enzyme-catalyzed reactions and assumed to follow the Michaelis-Menten kinetics (see Eqs. 1–2 in Supporting Material).

Activated HIF-1 can induce production of VEGF, EPO, PHD and p21. We explicitly characterize the induction of p21 and PHD with the Hill function (Eqs. 3 and 4), while implicating the roles for VEGF and EPO in the cellular adaptation to hypoxia. The HIF-1-PHD negative feedback promotes the adaptation of cells to mild hypoxia^{25,26}. PHD is divided into inactive (PHD) and active (PHD_a) forms, and their conversion depends on oxygen concentration (Eq. 6).

Activation of ATR. In severe hypoxia, the ribonucleotide reductase activity declines, leading to production of single-stranded DNA (ss-DNA) at stalled replication forks. ss-DNA is then coated with replication protein A (RPA), and the ATR-ATRIP (ATR interacting protein) complex is recruited to ss-DNA, which promotes ATR phosphorylation at T1989²⁷. ATR phosphorylation enhances its interaction with TopBP1, which further activates the kinase activity of ATR. Thus, the activation of ATR is positively regulated.

ATR is divided into ATR (inactive) and ATR_p (active), and their dynamics are described by Eqs. 7–8. The total level of ATR is assumed to be constant since ATR is mainly regulated posttranslationally²⁷. The phosphorylation and dephosphorylation of ATR are characterized by the Michaelis-Menten kinetics²⁸. The parameters are set to ensure that most of ATR is inactive in normoxia or mild hypoxia and ATR is quickly activated under severe hypoxia²⁹.

Regulation of p53 activity. p53 is degraded by Mdm2, which is induced by p53. ATR_p inhibits Mdm2 activity by phosphorylating it at Ser407³⁰ and disrupts the p53-Mdm2 interaction by phosphorylating p53 at Ser15, thereby leading to p53 accumulation²⁹. Based on its posttranslational modifications, nuclear p53 is divided into three forms: p53 (unphosphorylated), p53_p (phosphorylated), and p53_{pac} (phosphorylated and acetylated). Four forms of Mdm2 are defined here: Mdm2_c (cytoplasmic unphosphorylated), Mdm2_{cp} (cytoplasmic phosphorylated), Mdm2_n (nuclear unphosphorylated), and Mdm2_{np} (nuclear phosphorylated). For simplicity, we assume that only Mdm2_{cp} can enter the nucleus³¹. Mdm2_{np} cannot act as an E3 ubiquitin ligase³⁰.

The coactivator p300 is required for the full transcriptional activity of p53 and HIF-1. Their competition for binding to p300 is characterized by the Michaelis-Menten kinetics with competitive inhibition (see Eqs. 1–2 and 10–11). The acetylation rate of p53_p (or HIF-1 α) is an increasing function of its own concentration, and is a decreasing function of the level of HIF-1 α (or p53_p). On the other hand, p53, p53_p and HIF-1 α are targeted for degradation by Mdm2. The involved competition is also characterized by the Michaelis-Menten kinetics (Eqs. 1, 9 and 10). Notably, Mdm2-mediated degradation of p53_{pac} is neglected since its dual modifications block their interaction. p53-induced expression of target genes, including *mdm2* and *puma*, is all characterized by the Hill function, and the Hill coefficient is set to 4 given the p53 tetramer acts as a transcription factor.

Mdm2_c can be phosphorylated by Akt, promoting its nuclear entry³². Akt is activated via phosphorylation by PIP3 (phosphatidylinositol 3,4,5-trisphosphate), which is dephosphorylated by PTEN (phosphatase and tensin homolog) into PIP2 (phosphatidylinositol-4, 5-bisphosphate). The phosphorylation and dephosphorylation of Mdm2, Akt and PIP2/3 are all characterized by the Michaelis-Menten kinetics (Eqs. 12–15, 17 and 19). The total amount of Akt and that of PIP2 and PIP3 are separately assumed to be constant, similar to ref. 33.

Induction of apoptosis by p53. Different mechanisms have been proposed for p53-induced apoptosis in response to hypoxia. On one hand, repression of miR-17-92 by p53 is important for apoptosis induction since this relieves some proapoptotic genes such as *pten* and *bim* from the inhibition by miR-17-92^{12,34}. FOXO (forkhead box protein class O) is a typical transcription factor of *bim*, and its transcriptional activity is inhibited indirectly by Akt via phosphorylation³⁵. On the other hand, p53 also induces apoptosis by directly transactivating some proapoptotic genes such as *puma* and *fas*^{13,14}.

Here, we assume that p53 indirectly upregulates BIM and PTEN by transrepressing miR-17-92 in severe hypoxia or anoxia and directly induces PUMA in anoxia. There are two forms of FOXO: FOXO (active) and FOXO_p (phosphorylated, inactive), and Akt promotes the conversion from FOXO to FOXO_p. High expression of either BIM or PUMA promotes the release of cytochrome c (CytoC) from mitochondria, resulting in the activation of Caspase-3 (Casp3)³⁶. A positive feedback exists between CytoC release

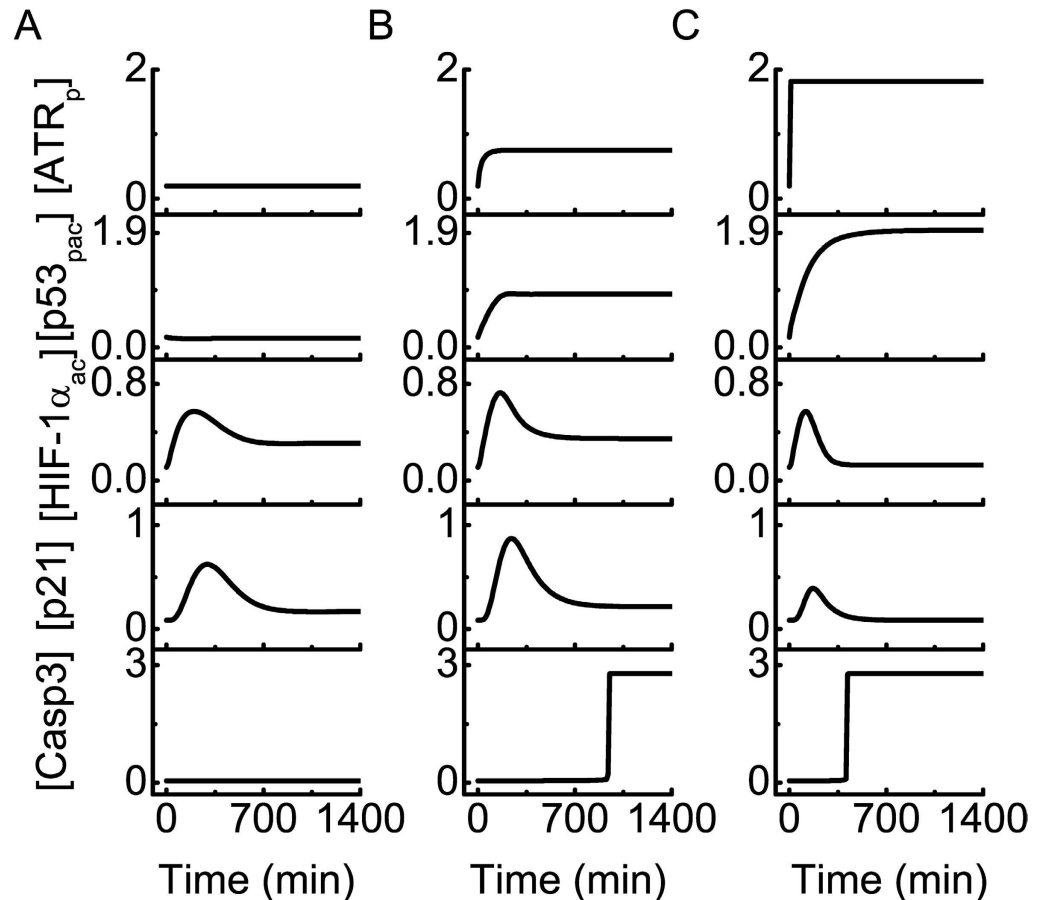


Figure 2. Overview of the network dynamics under different hypoxic conditions. Temporal evolution of the levels of ATR_p , $p53_{pac}$, $HIF-1\alpha_{ac}$, $p21$ and $Casp3$ in mild hypoxia (2% O_2 , (A)), severe hypoxia (0.02% O_2 , (B)), or anoxia (0% O_2 , (C)).

and $Casp3$ activation³⁷. The dynamics of CytoC and $Casp3$ are characterized in a similar manner to that in ref. 9 (Eqs. 26 and 27). The sustained activation of $Casp3$ is taken as the marker of apoptosis here.

Results

Overview of the dynamics of the HIF-1 α and p53 pathways. To illustrate the typical dynamics of the HIF-1 α and p53 pathways, we present the temporal evolution of protein concentrations under various hypoxic conditions in Fig. 2 ([...] denotes the concentration of each component throughout the paper). In mild hypoxia (2% O_2), $[p53_{pac}]$ is at a basal level because ATR is inactivated, and thus $Casp3$ remains inactive (Fig. 2A). $[HIF-1\alpha_{ac}]$ gradually rises and drops to an intermediate level, since PHD is induced by HIF-1 to promote the degradation of HIF-1 α (see Supplemental Fig. S1). $p21$ is induced by HIF-1 rather than p53 to trigger cell-cycle arrest. Consequently, the cell survives and adapts to mild hypoxia.

Under severe hypoxia (0.02% O_2), ATR is partly activated, and $[p53_{pac}]$ rises to an intermediate level (Fig. 2B). As a result, $[HIF-1\alpha_{ac}]$ first rises and then drops to a moderate level since $p53_p$ and HIF-1 α compete for binding to limiting p300. $p53_{pac}$ represses the expression of miR-17-92 to relieve the inhibition of BIM expression, and $[BIM]$ rises gradually to a relatively high level (see Supplemental Fig. S2). Since $[p53_{pac}]$ is not high enough, PUMA only accumulates to a low level. Consequently, $Casp3$ is activated mainly by BIM around 16 h and apoptosis ensues. These results are consistent with the experimental report that p53 can induce apoptosis via transrepressing antiapoptotic genes^{12,34}.

Under anoxia (0.0% O_2), ATR is fully activated and $[p53_{pac}]$ rises quickly to a high level (Fig. 2C). Because HIF-1 α is degraded by Mdm2 and p300 is mostly associated with p53, $[HIF-1\alpha_{ac}]$ returns to its basal level after a transient. Both $[BIM]$ and $[PUMA]$ rise to high levels, and $Casp3$ is activated around 6 h, which remarkably advances the induction of apoptosis.

The above results indicate that the cellular outcome depends on the extent of hypoxia (note that the hypoxic state is maintained persistently here). In mild hypoxia, $[HIF-1\alpha_{ac}]$ settles at an intermediate level, and the cell adapts to the stress after a transient cell-cycle arrest. Under severe hypoxia, the accumulation of $p53_{pac}$ suffices to elevate BIM via downregulating miR-17-92, and apoptosis is induced. In

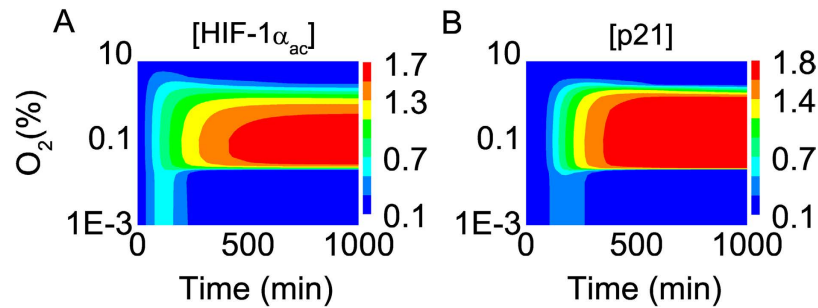


Figure 3. Dynamics of HIF-1 α_{ac} and p21. Color-coded concentrations of (A) HIF-1 α_{ac} and (B) p21 as a function of the logarithm of oxygen concentration and time.

anoxia, the stabilization and transcriptional activity of p53 are markedly enhanced, in sharp contrast to those of HIF-1 α . Both transcriptional repression and activation of target genes by p53 are triggered to expedite apoptosis induction, which awaits experimental validation. Notably, the competition for binding to limiting p300 is a key factor modulating the dynamics and activities of p53 and HIF-1 α .

Dynamics of HIF-1 α and p21. To investigate the dynamics of HIF-1 α and p21 systematically, we plot the heat maps of [HIF-1 α_{ac}] and [p21] as a function of oxygen concentration and time (Fig. 3). In normoxia (above 3% O₂), [HIF-1 α_{ac}] remains at basal levels since most of HIF-1 α is degraded (Fig. 3A). In mild hypoxia (between 1.1% and 3% O₂), [HIF-1 α_{ac}] gradually rises and drops due to PHD-dependent degradation. In moderate hypoxia (between 0.03% and 1.1% O₂), [HIF-1 α_{ac}] rises to different plateau levels, which can be as high as 1.6. p21 dynamics closely follow the dynamics of HIF-1 α_{ac} (Fig. 3B). These results suggest that the cell undergoes a transient cell-cycle arrest in mild hypoxia, or becomes senescent under moderate hypoxia because of sustained p21 induction. It would be interesting to test the occurrence of senescence.

In severe hypoxia (below 0.03% O₂), HIF-1 α first accumulates because of PHD deactivation; then, p53 competes with HIF-1 α for binding to p300, leading to a reduction in HIF-1 α_{ac} levels and inhibition of HIF-1 α activity. In anoxia, p53 competitively binds to p300 and Mdm2 targets HIF-1 α for degradation; thus, the HIF-1 α_{ac} level drops markedly, and rather low levels of p21 are induced. These results are consistent with the experimental observation that Mdm2 promotes HIF-1 α degradation in a p53-dependent way²². Together, HIF-1 α is partly inactivated under severe hypoxia and is degraded in anoxia.

p53 dynamics and apoptosis induction under severe hypoxia. Under severe hypoxia, ATR is activated, and thus p53 is stabilized by phosphorylation. For oxygen concentration below 0.025%, [ATR_p] quickly rises to plateau levels (Fig. 4A). ATR is partly activated when oxygen concentration is between 0.01% and 0.025%, or is fully activated when oxygen concentration is below 0.01%. Compared with ATR_p, p53_{pac} accumulates more slowly. The steady-state level of p53_{pac} rises with decreasing oxygen concentration (Fig. 4B). Of note, we can compare the simulation results with the experimental observations in ref. 8; for comparison, the measured p53 expression level is divided by its maximum (see Supplemental Fig. S3). p53_{pac} accumulates markedly only in severe hypoxia or anoxia, consistent with the experimental result, and the simulation results reproduce the key features of p53 dynamics in response to hypoxia.

Activated p53 represses miR-17-92 expression to upregulate BIM; [BIM] rises to distinct levels depending on oxygen concentration (Fig. 4C). In contrast, only when oxygen concentration is below 0.01% can [PUMA] rise to relatively high levels (Fig. 4D), consistent with the experimental observation¹³. Thus, the transrepression activity of p53 is activated in severe hypoxia, while its transactivation activity is further evoked under anoxia.

Either BIM or PUMA activates Casp3 to trigger apoptosis in hypoxia. The timing of Casp3 activation, T_{Apop} , versus oxygen concentration is shown in Fig. 4E. Casp3 can be activated around 400 min if oxygen concentration is below 0.015%; otherwise, T_{Apop} rises quickly with increasing oxygen concentration. Apoptosis cannot be induced when oxygen concentration is above 0.022%. As seen in Fig. 4F, the timing of Casp3 activation exhibits a significant delay with increasing oxygen concentration. Together, the cell becomes more sensitive to apoptosis with aggravating hypoxia.

Interplay between HIF-1 α and p53 under anoxia. As mentioned above, p53 and HIF-1 α compete for limiting p300 to activate their transcriptional activity and are targeted for degradation by Mdm2. Here, we explore their interplay under anoxia. We first investigate how the p300 level influences the steady-state concentrations of proteins (Fig. 5A). With increasing [p300], [p53_{pac}] continuously rises toward saturation. [Mdm2_n] remains at a low level over a wide range since Mdm2_{np} predominates in the nucleus. Intriguingly, [HIF-1 α_{ac}] first rises, then drops, and rises again with increasing [p300]. Since ATR is fully activated and [p53_p] is large enough under anoxia, increasing [p300] leads to enhancement of p53 acetylation. When [p300] is very low, the level of unacetylated HIF-1 α is sufficiently high, and

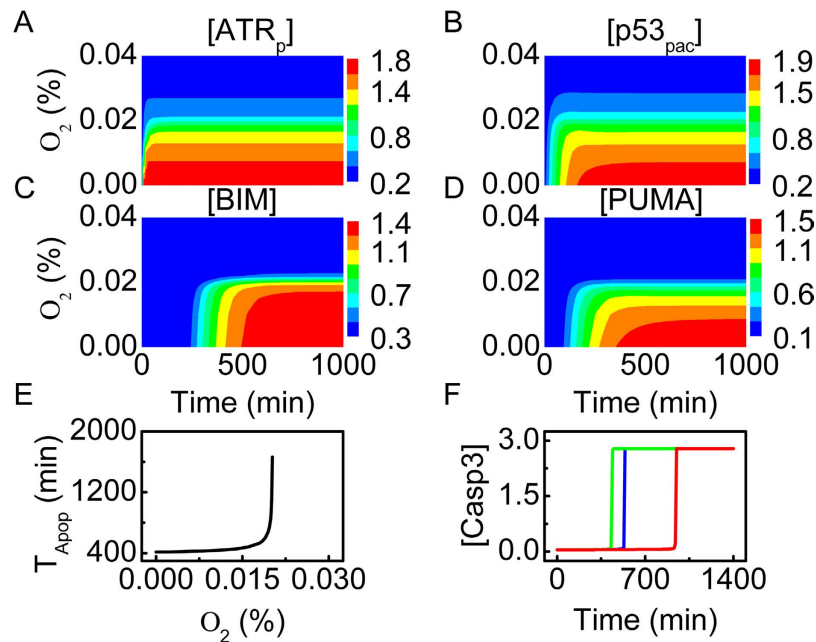


Figure 4. Protein dynamics and apoptosis induction under severe hypoxia. (A–D) Color-coded concentrations of ATR_p (A), $p53_{pac}$ (B), BIM (C) and PUMA (D) as a function of oxygen concentration and time. (E) The timing of Casp3 activation versus oxygen concentration. (F) Time courses of $[Casp3]$ with oxygen concentration at 0.01% (green), 0.018% (blue), or 0.02% (red).

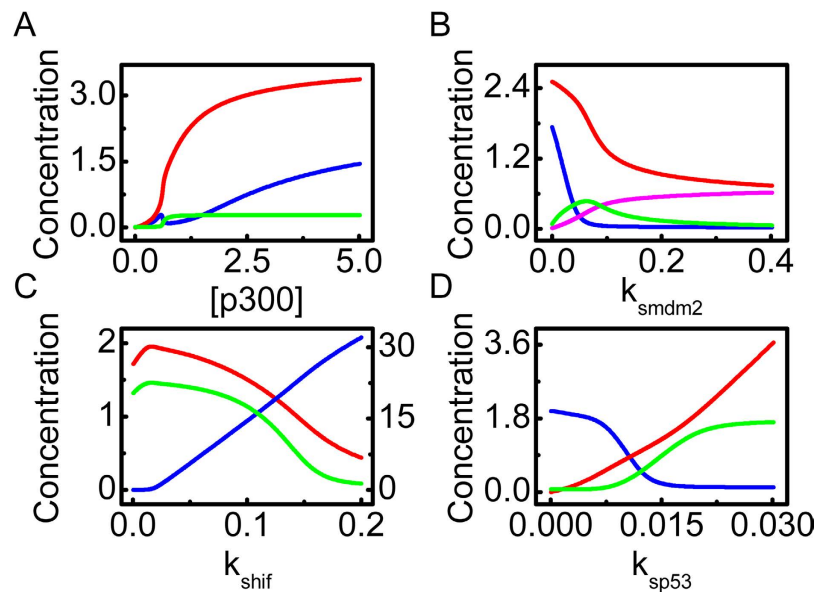


Figure 5. Interplay between HIF-1 α and p53 in anoxia. (A) Bifurcation diagrams of $[p53_{pac}]$ (red), $[HIF-1\alpha_{ac}]$ (blue) and $[Mdm2_n]$ (green) versus the amount of p300. (B) Bifurcation diagrams of $[p53_{pac}]$ (red), $[HIF-1\alpha_{ac}]$ (blue), $[Mdm2_c]$ (green) and $[Mdm2_n]$ (pink) versus the p53-induced production rate of Mdm2, k_{smdm2} . (C) Bifurcation diagrams of $[HIF-1\alpha_{ac}]$ (blue, on the right axis), $[p53_{pac}]$ (red) and $[PUMA]$ (green) versus the production rate of HIF-1 α , k_{shif} . (D) Bifurcation diagrams of $[HIF-1\alpha_{ac}]$ (blue), $[p53_{pac}]$ (red) and $[PUMA]$ (green) versus the production rate of p53, k_{sp53} .

$[HIF-1\alpha_{ac}]$ rises with increasing $[p300]$. When $[p300]$ further rises, $[p53_{pac}]$ is elevated and HIF-1 α is markedly degraded by p53-induced Mdm2, leading to a drop in $[HIF-1\alpha_{ac}]$. If p300 is in excess, more HIF-1 α is acetylated, resulting in a continuous rise in $[HIF-1\alpha_{ac}]$ with increasing $[p300]$. The intricate effect of p300 level on the acetylation of HIF-1 α is worth testing experimentally.

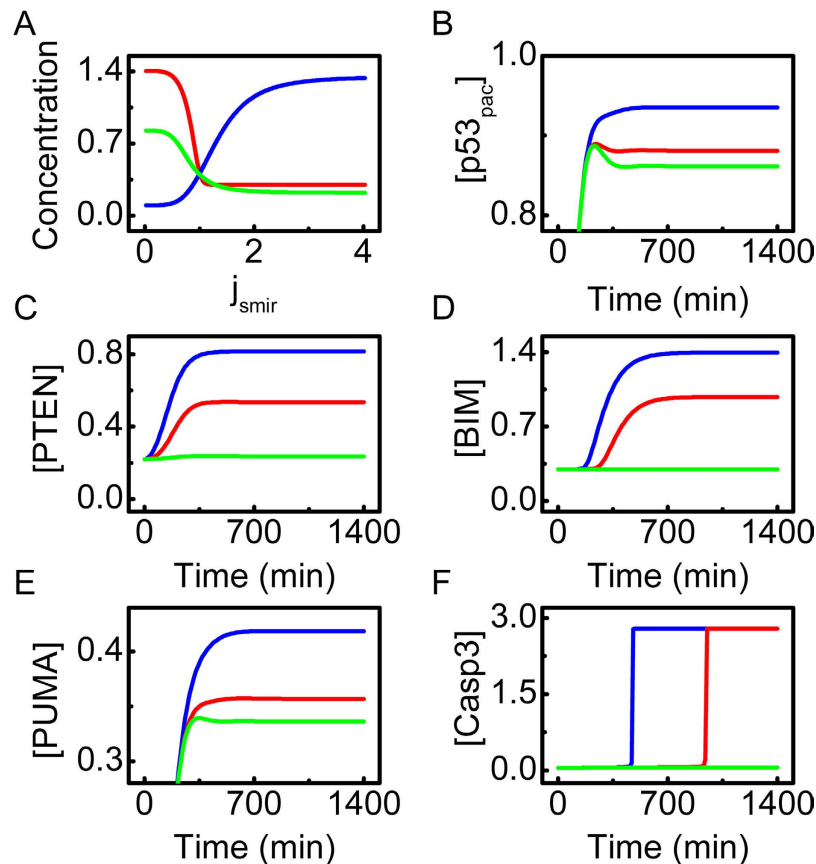


Figure 6. Effect of miR-17-92 on apoptosis induction under severe hypoxia (0.02% O₂). (A) Bifurcation diagrams of [PTEN] (green), [BIM] (red) and [miR-17-92] (blue) as a function of j_{smir} . (B–F) Time courses of [p53_{pac}] (B), [PTEN] (C), [BIM] (D), [PUMA] (E) and [Casp3] (F) with $j_{smir} = 0.3$ (blue), 0.8 (red), or 2.0 (green).

We further probe the role for Mdm2-mediated degradation of p53 and HIF-1 α . With increasing the p53-induced production rate of Mdm2, k_{smdm2} , [HIF-1 α_{ac}] first drops fast and then remains at basal levels because of enhanced degradation of HIF-1 α by Mdm2 (Fig. 5B). In contrast, [p53_{pac}] falls at a slower rate and always remains above an intermediate level. At large k_{smdm2} , Mdm2_n predominates over Mdm2_c since [p53_{pac}] is not sufficiently high to transrepress miR-17-92 markedly, which promotes the nuclear entry of Mdm2. Collectively, Mdm2 overexpression inhibits the transcriptional activities of both HIF-1 and p53.

The expression level of HIF-1 α has a marked effect on the activities of HIF-1 α and p53. The amount of HIF-1 α depends on its production rate k_{shif} . For very low k_{shif} [p53_{pac}] remains at high levels, whereas there is little amount of HIF-1 α_{ac} (Fig. 5C). When k_{shif} is further increased, more HIF-1 α is produced and [HIF-1 α_{ac}] gradually rises, leading to a drop in [p53_{pac}] because of their competition for limiting p300. Since PUMA expression is p53-dependent, [PUMA] shows the similar dynamics to [p53_{pac}]. Thus, p53 cannot be activated to induce apoptosis even under anoxia when HIF-1 α is overexpressed.

Similarly, the p53 expression level affects the activities of HIF-1 α and p53. With increasing the rate constant of p53 production, k_{sp53} , [p53_{pac}] rises continuously, whereas [HIF-1 α_{ac}] drops to basal levels (Fig. 5D). As a result, [PUMA] gradually rises toward saturation at large k_{sp53} . Of note, [HIF-1 α_{ac}] remains at high levels with $k_{sp53}=0$, and apoptosis cannot be induced even in anoxia. This result is consistent with the fact that cells with p53 mutation are resistant to proapoptotic stimuli³⁸. Together, the competition between p53 and HIF-1 α for p300 and Mdm2 plays a key role in the modulation of their stabilization and transcriptional activity.

Effect of miR-17-92 repression on apoptosis induction. In addition to repression of FOXO-induced BIM expression, miR-17-92 also indirectly suppresses FOXO and p53 activities by inhibiting PTEN expression³⁰. Here, we clarify the significance of miR-17-92 inhibition by p53 in hypoxia-induced apoptosis. Note that the parameter j_{smir} characterizes the repression strength by p53: the larger j_{smir} the weaker the repression becomes (see Eq. 21).

As shown in the bifurcation diagrams, [PTEN] and [BIM] remain at relatively high levels for $j_{smir} \leq 1$, whereas [miR-17-92] is at low levels (Fig. 6A). In contrast, [PTEN] and [BIM] stay at low levels once $j_{smir} > 1$, whereas [miR-17-92] gradually rises with increasing j_{smir} . This suggests that the effective

transrepression of miR-17-92 by p53 is indispensable for apoptosis induction under severe hypoxia, which awaits experimental validation.

We further show the temporal evolution of protein concentrations for different values of j_{smir} in Fig. 4B–F. At $j_{\text{smir}} = 0.3$, [PTEN] reaches a high level, promoting the accumulation of p53. High expression of BIM and PUMA activates Casp3 to trigger apoptosis promptly. If j_{smir} is increased to 0.8, the expression of PTEN and BIM is reduced, and the levels of p53_{pac} and PUMA are downregulated. Consequently, Casp3 is activated with a marked delay. At $j_{\text{smir}} = 2.0$, the repression of miR-17-92 expression by p53 becomes very weak, and apoptosis cannot be induced. Collectively, the transrepression of miR-17-92 is significant for apoptosis induction under severe hypoxia.

Discussion

In this work, we provide a coherent picture of cell-fate decision under hypoxic conditions. Under normoxia, both HIF-1 α and p53 are at very low levels. In mild hypoxia, p53 still remains inactive, whereas HIF-1 α first accumulates to induce transient cell-cycle arrest and then settles at moderate levels because of the cellular adaptation to hypoxia. Under moderate hypoxia, HIF-1 α_{ac} expression is sufficiently high, and p21 induction is maintained to trigger cellular senescence. In severe hypoxia, p53 accumulation attenuates HIF-1 α activity, and p53 transrepresses antiapoptotic genes like miR-17-92 to relieve inhibition of proapoptotic genes like BIM, thereby inducing apoptosis. Under anoxia, high levels of p53 lead to HIF-1 α degradation, and p53 transrepresses and transactivates target genes to remarkably advance apoptosis induction. Such a decision mechanism seems plausible, either promoting cellular adaptation to mild stress or inducing cell death after severe stress.

The interplay between p53 and HIF-1 α plays a key role in the hypoxic response. Our results are consistent with experimental observations: moderate p53 expression attenuates HIF-1 α activity, whereas high p53 expression eliminates HIF-1 α activity³⁹. Notably, HIF-1 α is overexpressed in most cancers⁴⁰, and thus developing HIF-1 α inhibitors to prevent the adaptation of tumor cells to hypoxia may be a promising strategy for anticancer⁴¹. Our results suggest that reactivation of p53 could contribute to inhibition of HIF-1 α activity.

The mechanism for p53 stabilization is somehow controversial in the literature. Previously, it was reported that p53 was stabilized by HIF-1 α ¹⁶. Later, this mechanism was challenged by the report that p53 accumulated only in severe hypoxia⁸. Thus, HIF-1 α alone cannot stabilize p53. Rather, it was found that ATR contributes to p53 stabilization in severe hypoxia when replication arrest occurs. Here, we further show that the competition between p53 and HIF-1 α for limiting p300 not only determines their transcriptional activity, but also regulates their abundance because p300-mediated acetylation prevents Mdm2-mediated protein degradation. p53 stabilization is enhanced when more Mdm2 is associated with unacetylated HIF-1 α .

Our work may reconcile the contradictory reports on the mechanism for hypoxia-induced apoptosis^{11–13}. We propose that depending on the severity of hypoxia, p53 may suppress the expression of antiapoptotic genes like miR-17-92, or inhibit miR-17-92 expression and activate PUMA expression synergistically to induce apoptosis. Accordingly, it takes a relatively long time to evoke apoptosis under severe hypoxia, or apoptosis is induced promptly after exposure to anoxia. Such an action mode of p53 is of functional significance, allowing for cellular adaptation to the hypoxic environment or eliminating cells promptly under strongly anoxic conditions. It would be interesting to experimentally test that.

We showed that effective repression of miR-17-92 expression is required for apoptosis induction under severe hypoxia. miR-17-92 itself can inhibit the production of BIM and PTEN³⁴. Conversely, p53 transrepresses miR-17-92 to elevate BIM and PTEN expression¹². BIM can induce apoptosis⁴², while PTEN contributes to p53 stabilization by sequestering Mdm2 in the cytoplasm³². It is worthy to explore whether other microRNAs induced by p53, such as miR-34a, contribute to apoptosis induction in hypoxia.

Finally, it is worth noting that the cellular response to hypoxia is extremely complicated. Here, we took a simplified approach to characterize the crosstalk between HIF-1 α and p53 signaling by focusing on their competition in stabilization and transcriptional activity. We probed the effect of the severity of hypoxia on cell fate, while omitting the influence of the duration of hypoxia. Some other factors were also ignored, such as complex relationships between HIF-1, p53 and pVHL⁷ and different phosphorylation modifications of p53. Definitely, adding more facets of signal transduction to the model should shed new light on the hypoxic response.

Methods

The details of the model are presented in the Supporting Material. The concentration of each component is represented by a dimensionless state variable. The temporal evolution of dynamic systems is governed by ordinary differential equations, which are presented in Supplemental Method. All the initial values of variables are their lower steady-state values under normoxia and are listed in Supplemental Table S1. The standard parameter values are listed in Supplemental Table S2. Some parameters are set based on experimental measurements or known facts, while others are estimated by comparing the simulation results with experimental data. The unit of time is minutes, while the units of parameters are determined such that the concentrations of proteins are dimensionless. For simplicity, we do not indicate the units of the parameters explicitly. The rate equations are numerically solved using Oscill8.

The robustness of protein concentrations to parameter variations is also analyzed, and the results are presented in Supplemental Table S3. The sensitivity of steady-state levels of HIF-1 α_{ac} and p53 $_{pac}$ to parameter variations is calculated when the parameter values are varied by $\pm 10\%$ with respect to their standard values. These concentrations are only sensitive to the parameters related to HIF-1 α regulation, Mdm2-mediated protein degradation, or p53 production. Overall, our simulation results are robust to changes in most parameters, and we provide a model for effectively exploring the interplay between p53 and HIF-1 α in response to hypoxia.

References

1. Semenza, G. L. HIF-1: Upstream and downstream of cancer metabolism. *Curr. Opin. Genet. Dev.* **20**, 51–56 (2010).
2. Wang, G. L., Jiang, B. H., Rue, E. A. & Semenza, G. L. Hypoxia-inducible factor 1 is a basic-helix-loop-helix-PAS heterodimer regulated by cellular O₂ tension. *Proc. Natl. Acad. Sci. USA* **92**, 5510–5514 (1995).
3. Ivan, M. *et al.* HIF α targeted for VHL-mediated destruction by proline hydroxylation: Implications for O₂ sensing. *Science* **292**, 464–468 (2001).
4. Lando, D. *et al.* FIH-1 is an asparaginyl hydroxylase enzyme that regulates the transcriptional activity of hypoxia-inducible factor. *Genes Dev.* **16**, 1466–1471 (2002).
5. Semenza, G. L. Targeting HIF-1 for cancer therapy. *Nat. Rev. Cancer* **3**, 721–732 (2003).
6. Greer, S. N., Metcalf, J. L., Wang, Y. & Ohh, M. The updated biology of hypoxia-inducible factor. *EMBO J.* **31**, 2448–2460 (2012).
7. Sermeus, A. & Michiels, C. Reciprocal influence of the p53 and the hypoxic pathways. *Cell Death Dis.* **2**, e164 (2011).
8. Hammond, E. M., Denko, N. C., Dorie, M. J., Abraham, R. T. & Giaccia, A. J. Hypoxia links ATR and p53 through replication arrest. *Mol. Cell. Biol.* **22**, 1834–1843 (2002).
9. Zhang, X. P., Liu, F. & Wang, W. Two-phase dynamics of p53 in the DNA damage response. *Proc. Natl. Acad. Sci. USA* **108**, 8990–8995 (2011).
10. Fridman, J. S. & Lowe, S. W. Control of apoptosis by p53. *Oncogene* **22**, 9030–9040 (2003).
11. Koumenis, C. *et al.* Regulation of p53 by hypoxia: Dissociation of transcriptional repression and apoptosis from p53-dependent transactivation. *Mol. Cell. Biol.* **21**, 1297–1310 (2001).
12. Yan, H. L. *et al.* Repression of the miR-17-92 cluster by p53 has an important function in hypoxia-induced apoptosis. *EMBO J.* **28**, 2719–2732 (2009).
13. Yu, J., Wang, Z., Kinzler, K. W., Vogelstein, B. & Zhang, L. PUMA mediates the apoptotic response to p53 in colorectal cancer cells. *Proc. Natl. Acad. Sci. USA* **100**, 1931–1936 (2003).
14. Liu, T. *et al.* Hypoxia induces p53-dependent transactivation and Fas/CD95-dependent apoptosis. *Cell Death Differ.* **14**, 411–421 (2006).
15. Fei, P. *et al.* Bnip3L is induced by p53 under hypoxia, and its knockdown promotes tumor growth. *Cancer Cell* **6**, 597–609 (2004).
16. An, W. G. *et al.* Stabilization of wild-type p53 by hypoxia-inducible factor 1 α . *Nature* **392**, 405–408 (1998).
17. Chen, D., Li, M., Luo, J. & Gu, W. Direct interactions between HIF-1 α and Mdm2 modulate p53 function. *J. Biol. Chem.* **278**, 13595–13598 (2003).
18. Schmid, T., Zhou, J., Köhl, R. & Brüne, B. p300 relieves p53-evoked transcriptional repression of hypoxia-inducible factor-1 (HIF-1). *Biochem. J.* **380**, 289–295 (2004).
19. Qutub, A. A. & Popel, A. S. A computational model of intracellular oxygen sensing by hypoxia-inducible factor HIF1 α . *J. Cell Sci.* **119**, 3467–3480 (2006).
20. Schmierer, B., Novák, B. & Schofield, C. J. Hypoxia-dependent sequestration of an oxygen sensor by a widespread structural motif can shape the hypoxic response - a predictive kinetic model. *BMC Syst. Biol.* **4**, 139 (2010).
21. Nguyen, L. K. *et al.* A dynamic model of the hypoxia-inducible factor 1 α (HIF-1 α) network. *J. Cell Sci.* **126**, 1454–1463 (2013).
22. Ravi, R. *et al.* Regulation of tumor angiogenesis by p53-induced degradation of hypoxia-inducible factor 1 α . *Genes Dev.* **14**, 34–44 (2000).
23. Arany, Z. *et al.* An essential role for p300/CBP in the cellular response to hypoxia. *Proc. Natl. Acad. Sci. USA* **93**, 12969–12973 (1996).
24. Avantaggiati, M. L. *et al.* Recruitment of p300/CBP in p53-dependent signal pathways. *Cell* **89**, 1175–1184 (1997).
25. D'Angelo, G., Duplan, E., Boyer, N., Vigne, P. & Frelin, C. Hypoxia up-regulates prolyl hydroxylase activity: A feedback mechanism that limits HIF-1 responses during reoxygenation. *J. Biol. Chem.* **278**, 38183–38187 (2003).
26. Stiehl, D. P. *et al.* Increased prolyl 4-hydroxylase domain proteins compensate for decreased oxygen levels: Evidence for an autoregulatory oxygen-sensing system. *J. Biol. Chem.* **281**, 23482–23491 (2006).
27. Liu, S. *et al.* ATR autophosphorylation as a molecular switch for checkpoint activation. *Mol. Cell* **43**, 192–202 (2011).
28. Kholodenko, B. N. Cell-signalling dynamics in time and space. *Nat. Rev. Mol. Cell Biol.* **7**, 165–176 (2006).
29. Hammond, E. M., Dorie, M. J. & Giaccia, A. J. ATR/ATM targets are phosphorylated by ATR in response to hypoxia and ATM in response to reoxygenation. *J. Biol. Chem.* **278**, 12207–12213 (2003).
30. Shinozaki, T., Nota, A., Taya, A. & Okamoto, K. Functional role of Mdm2 phosphorylation by ATR in attenuation of p53 nuclear export. *Oncogene* **22**, 8870–8880 (2003).
31. Mayo, L. D. & Donner, D. B. A phosphatidylinositol 3-kinase/Akt pathway promotes translocation of Mdm2 from the cytoplasm to the nucleus. *Proc. Natl. Acad. Sci. USA* **98**, 11598–11603 (2001).
32. Manning, B. D. & Cantley, L. C. AKT/PKB signaling: Navigating downstream. *Cell* **129**, 1261–1274 (2007).
33. Wee, K. B. & Aguda, B. D. Akt versus p53 in a network of oncogenes and tumor suppressor genes regulating cell survival and death. *Biophys. J.* **91**, 857–865 (2006).
34. Xiao, C. *et al.* Lymphoproliferative disease and autoimmunity in mice with increased miR-17-92 expression in lymphocytes. *Nat. Immunol.* **9**, 405–414 (2008).
35. Kloet, D. E. A. & Burgering, B. M. T. The PKB/FOXO switch in aging and cancer. *BBA-Mol. Cell Res.* **1813**, 1926–1937 (2011).
36. Cory, S. & Adams, J. M. The Bcl2 family: Regulators of the cellular life-or-death switch. *Nat. Rev. Cancer* **2**, 647–656 (2002).
37. Kirsch, D. G. *et al.* Caspase-3-dependent cleavage of Bcl-2 promotes release of cytochrome c. *J. Biol. Chem.* **274**, 21155–21161 (1999).
38. Levine, A. J. p53, the cellular gatekeeper for growth and division. *Cell* **88**, 323–331 (1997).
39. Schofield, C. J. & Ratcliffe, P. J. Oxygen sensing by HIF hydroxylases. *Nat. Rev. Mol. Cell Biol.* **5**, 343–354 (2004).
40. Talks, K. L. *et al.* The expression and distribution of the hypoxia-inducible factors HIF-1 α and HIF-2 α in normal human tissues, cancers, and tumor-associated macrophages. *Am. J. Pathol.* **157**, 411–421 (2000).
41. Xia, Y., Choi, H. K. & Lee, K. Recent advances in hypoxia-inducible factor (HIF)-1 inhibitors. *Eur. J. Med. Chem.* **49**, 24–40 (2012).
42. Bouillet, P. *et al.* Proapoptotic Bcl-2 relative Bim required for certain apoptotic responses, leukocyte homeostasis, and to preclude autoimmunity. *Science* **286**, 1735–1738 (1999).

Acknowledgments

This work was supported by the 973 program of China (No. 2013CB834104), National Natural Science Foundation of China (Nos. 11175084, 11204126 and 31361163003), and PAPD.

Author Contributions

X.P.Z. and F.L. designed research; C.H.Z. performed numerical simulations; C.H.Z., X.P.Z., F.L. and W.W. analyzed data; C.H.Z., X.P.Z. and F.L. wrote the paper; F.L. coordinated the research. All authors reviewed the manuscript.

Additional Information

Supplementary information accompanies this paper at <http://www.nature.com/srep>

Competing financial interests: The authors declare no competing financial interests.

How to cite this article: Zhou, C.-H. *et al.* Modeling the interplay between the HIF-1 and p53 pathways in hypoxia. *Sci. Rep.* **5**, 13834; doi: 10.1038/srep13834 (2015).



This work is licensed under a Creative Commons Attribution 4.0 International License. The images or other third party material in this article are included in the article's Creative Commons license, unless indicated otherwise in the credit line; if the material is not included under the Creative Commons license, users will need to obtain permission from the license holder to reproduce the material. To view a copy of this license, visit <http://creativecommons.org/licenses/by/4.0/>